Electronic Supporting Information

Soft Nanoparticles as Antimicrobial Agents and Carriers of Microbiocides for Enhanced Inhibition Activity

Hui Wen Yong,[a] Seyed Mohammad Amin Ojagh, [a] Gabriel Théberge-Julien,[bc] Laura Sofia Reyes Castellanos,[a] Faiza Tebbji,[b] Theo G.M. van de Ven,[a] Adnane Sellam,[bc] Éric Rhéaume,[bc] Jean-Claude Tardif[# bc], and Ashok Kakkar[a]*

[a]Department of Chemistry, McGill University, 801 Sherbrooke Street West, Montréal, Québec, H3A 0B8 Canada. *ashok.kakkar@mcgill.ca

[b]Research Centre, Montréal Heart Institute, 5000 Belanger Street, Montréal, Québec H1T 1C8, Canada.[#]jean-claude.tardif@icm-mhi.org

[c]Department of Medicine, Université de Montréal, Montréal, Québec H3T 1J4, Canada.

1. Synthesis and characterization

Characterization

A Bruker AVIIIHD 500 MHz spectrometer was used to record all NMR spectra at ambient temperature. The spectra were calibrated at 7.26 ppm (^{1}H NMR)/ 77.16 ppm (^{13}C NMR) respectively in relation to the residual undeuterated solvent in chloroform-d. A Bruker MALDI Autoflex III TOF mass spectrometer controlled by Flex Analysis was used to acquire the mass spectra in linear positive ion mode. The presence of the azide group in PEG_{2050}-N_3 was confirmed using an Attenuated total reflectance- Fourier-transform infrared spectrometer (ATR-FTIR) spectrometer equipped with a single bounce diamond crystal and a $LiTaO_3$ detector. All measurements were conducted at room temperature from 400 to 4000 cm^{-1}. The number-average molecular weight (M_n) and polydispersity index ($Đ$) were determined using GPC with THF as an eluent. Measurements were performed on a Waters Breeze system equipped with 3 Waters Styragel HR columns (HR1 with a molar mass range of 100-5000 g mol^{-1}, HR2 with a molar mass range of 500-20000 g mol^{-1}, HR4 with a molar mass range of 5000-600000 g mol^{-1}) and a guard column. The flow rate was 0.3 mL min^{-1} (40 °C) while the standards used were polymethyl methacrylate (PMMA) standards (PSS Polymer Standards Service GmbH, molar masses ranging from 682 to 1520000 g mol-1). Sample detection and quantification were conducted with a differential refractive index detector (RI 2414). A Brookhaven Instrument NanoBrook Omni equipped with a 40-mW diode laser operating at 640 nm was used to obtain the hydrodynamic diameters, polydispersity index and zeta potential of micelles at room temperature. A Varian Cary Eclipse fluorescence spectrometer was used to measure the change in fluorescence intensities of pyrene at room temperature. A FEI Tecnai 12 BioTwin 120 kV transmission electron microscope (TEM) equipped with an AMT XR80 CCD Camera System located at the Facility for Electron Microscopy Research (FEMR) at McGill University was used to examine the morphologies of micelles. All solutions were stained with 2% uranyl acetate and left to dry overnight prior to analysis. The CUR and TBF standard curves, as well as the release studies were examined on a Varian Cary50 Ultraviolet-visible (UV-Vis) spectrophotometer equipped with a Xenon lamp at ambient temperature. A FEI Quanta 450 Environmental Scanning Electron Microscope (SEM) located at the FEMR was used to image the bacteria in the absence/ presence of micellar solutions. In general, the bacteria solutions were centrifuged at 14,000 rpm for 5 mins and the supernatant was replaced with 0.5 mL of 2.5% glutaraldehyde in PBS (0.1 M, pH 7.4). After dispersing the

bacteria in the fixative at 4 °C for 1 day, the bacteria were washed with 0.5 mL PBS twice before embedding on a poly(L-lysine) coated 12 mm glass slide. The samples were then dehydrated by immersing in increasing ethanol concentrations of 30%, 50%, 70%, 80%, 90%, 95% for 10 min each, and twice at 100% for an additional 10 min each. The solution was then dried in a Leica Microsystems EM CPD300 Critical Point Dryer before coating with platinum (5 nm) using a Leica Microsystems EM ACE600 High-Resolution Sputter Coater at room temperature.

Synthesis

Synthesis of α-tosyl-ω-hydroxyl PEG_{2050} (P1)

Fresh Ag_2O was first prepared by adding a 9 mL aqueous solution of NaOH (0.120 g, 3.00 mmol) at 85 ºC to a separate 2 mL aqueous solution of $AgNO_3$ (0.700 g, 4.12 mmol) at 85 ºC. The brown solid formed was collected and washed extensively with hot water and methanol before drying overnight under reduced pressure. PEG_{2050} (2.50 g, 1.22 mmol, 1 eq), Ag_2O (0.433 g, 1.87 mmol, 1.5 eq), KI (0.042 g, 0.25 mmol, 0.2 eq) and dry DCM were added into a 3-neck flask under nitrogen and cooled in an ice bath. In another flask, *p*-toluenesulfonyl chloride (0.250 g, 1.31 mmol, 1.05 eq) was dissolved in dry DCM before adding dropwise into the PEG_{2050} solution via an addition funnel. The reaction was stirred continuously under a nitrogen atmosphere and allowed to proceed at room temperature for 14 h. The final reaction mixture was then centrifuged at 3000 RPM for 10 min. The supernatant was concentrated and dropped in excess cold diethyl ether to precipitate the product. The product was filtered and dried under reduced pressure to yield a white powder. Yield: 92% (2.46 g). ^{1}H NMR (500 MHz, $CDCl_3$): δ (ppm) 2.43 (s, 3H, -CH_3), 2.74 (br s, 1H, OH), 3.62 (m, 180H, -(CH_2CH_2O)$_{44}$), 3.70 (t, 2H, -CH_2CH_2OH), 4.14 (t, 2H, CH_2OTs), 7.32 (d, 2H, -ArH), 7.77 (d, 2H, -ArH). ^{13}C{^{1}H} NMR (125 MHz, $CDCl_3$): δ_C (ppm) 21.8, 61.8, 68.8, 69.4, 70.4, 70.7, 70.9, 72.7, 128.1, 129.9, 133.2, 144.9.

Synthesis of α-azide-ω-hydroxyl PEG_{2050} (P2)

P1 (2.500 g, 1.11 mmol, 1 eq), NaN_3 (0.616 g, 9.48 mmol, 8 eq) and anhydrous ethanol were added to a round bottom flask under a nitrogen atmosphere. The reaction mixture was then refluxed at 85 °C with continuous stirring for 24 h. All the solvent was removed, and the crude product was dissolved in DCM. The solution was then washed 2 times with brine and another 2 times with water before drying with $MgSO_4$. After removing the drying agent, the product was concentrated

using a rotary evaporator and precipitated by dropwise addition to ice cold diethyl ether. The precipitate was then filtered before drying under reduced pressure to obtain a white solid product. Yield: 95% (2.2 g). ^{1}H NMR (500 MHz, $CDCl_3$): δ (ppm) 2.69 (s, 1H, -OH), 3.38 (t, 2H, -$CH_2CH_2N_3$), 3.64 (s, 180H, -($CH_2CH_2O)_{43}$), 3.71 (t, 2H, -$CH_2CH_2N_3$), 3.77 (t, 2H, -CH_2CH_2OH). ^{13}C{^{1}H} NMR (125 MHz, $CDCl_3$): *δ* (ppm) 50.8, 61.9, 70.2, 70.5, 70.7, 72.7.

Synthesis of Boc-NH-PEG_{2050}-N_3 (P3)

P2 (2 g, 0.956 mmol, 1 eq), *N*-(*tert*-Butoxycarbonyl)-4-aminobutyric acid (Boc-GABA-OH, 0.308 g, 1.43 mmol, 1.5 eq), DMAP (0.247 g, 1.91 mmol, 2 eq) and dry DCM were added into a round bottom flask under nitrogen. The flask was chilled to 0 °C. A separate solution of DCC (0.833 g, 3.82 mmol, 4 eq) in dry DCM was then added dropwise slowly into the flask under nitrogen. The reaction mixture was left to react for 24 h. Afterwards, dry DCM was removed completely, and the crude product was dissolved in acetone (10 mL). Any precipitate was then removed by vacuum filtration and the solution was concentrated and precipitated by dropwise addition to ice cold diethyl ether. The product was filtered before drying under reduced pressure to obtain a white solid product. Yield: 75% (1.60 g). ^{1}H NMR (500 MHz, $CDCl_3$): δ (ppm) 1.42 (s, 9H, -$C(CH_3)_3$), 1.81 (m, 2H, -$NHCH_2CH_2CH_2CO$), 2.38 (t, 2H, -$NHCH_2CH_2CH_2CO$), 3.15 (t, 2H, -$NHCH_2CH_2CH_2CO$), 3.38 (t, 2H, -$OCH_2CH_2N_3$), 3.49 (t, 2H, -$OCH_2CH_2N_3$), 3.63 (m, 180H, -($CH_2CH_2O)_{43}$), 3.77 (t, 2H, -$OCCH_2CH_2(CH_2CH_2O)_{43}$), 4.22 (t, 2H, -$OCCH_2CH_2(CH_2CH_2O)_{43}$), 4.72 (br s, 1 H, NH). ^{13}C{^{1}H} NMR (125 MHz, $CDCl_3$): δ (ppm) 28.5, 31.6, 50.8, 63.7, 69.2, 70.2, 70.8, 79.3, 156.1, 173.5.

Synthesis of 3,5- bis(prop-2-ynyloxy)benzyl polycaprolactone (P5)

P4 was synthesized as reported in Chapter 2. To a flask containing P4 (0.1 g, 0.463 mmol, 1 eq), dry toluene was added and heated to 100 °C under nitrogen with magnetic stirring. ε-caprolactone (1.8 mL, 16.2 mmol, 35 eq) was then added and the flask was further heated to 110 °C. Next, tin(II) 2-ethyl hexanoate (0.015 mL, 0.469 mmol, 0.1 eq) was added and the reaction mixture was refluxed at 115 °C for 24 h. Toluene was first evaporated off under reduced pressure and the crude product was dissolved in minimal DCM followed by precipitation in ice cold methanol. The product was collected and dried in a desiccator.

Yield= 83% (1.95 g). ^{1}H NMR (500 MHz, $CDCl_3$): δ (ppm) 1.35- 1.41 (m, 70H, (-$OCCH_2CH_2CH_2CH_2CH_2$-O)$_{33}$), 1.61- 1.68 (m, 136H, (-$OCCH_2CH_2CH_2CH_2CH_2O)_{33}$), 2.30 (t, 66H, (-$OCCH_2CH_2CH_2CH_2CH_2O)_{33}$), 2.54 (t, 2H, -C≡CH), 4.06 (t, 68H, (-$OCCH_2CH_2CH_2CH_2CH_2O)_{33}$), 4.68 (d, 4H, -$CH_2$C≡C), 5.06 (s, 2H, -Ar$CH_2$O), 6.57 (t, 1H, -ArH), 6.60 (d, 2H, -ArH). ^{13}C{^{1}H} NMR (125 MHz, $CDCl_3$): δ (ppm) 24.7, 25.7, 28.5, 34.4, 56.1, 62.8, 64.3, 65.9, 75.9, 78.4, 101.9, 107.6, 158.9, 173.7. MS: MALDI-ToF M_n = 3411.83; M_w = 3478.16; PDI = 1.02; DP = 30.

2. Supplementary Figures

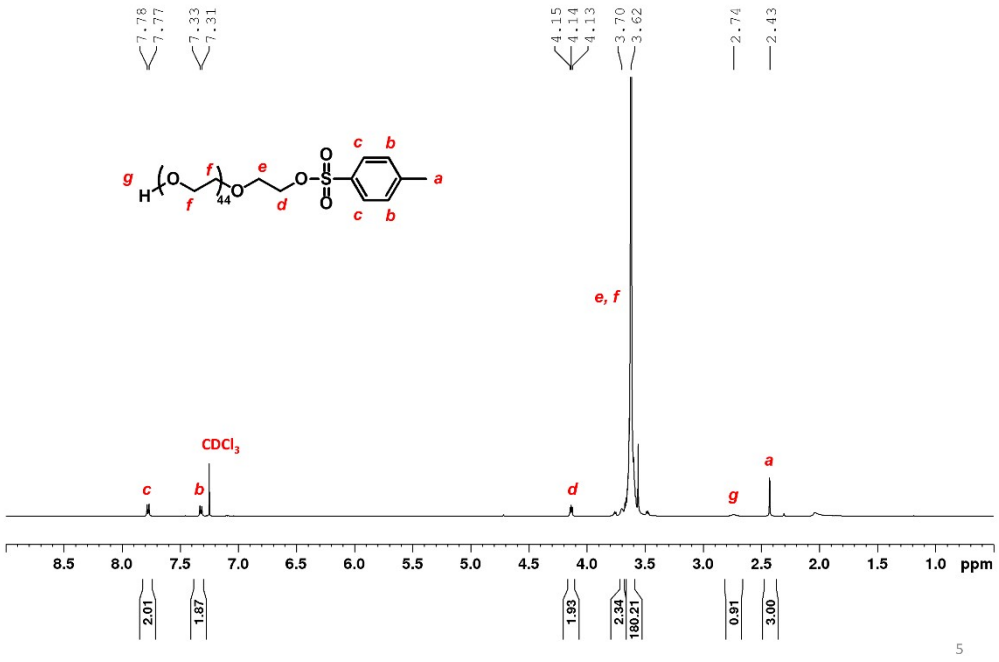

Fig. S1 ^{1}H NMR spectrum of P1.

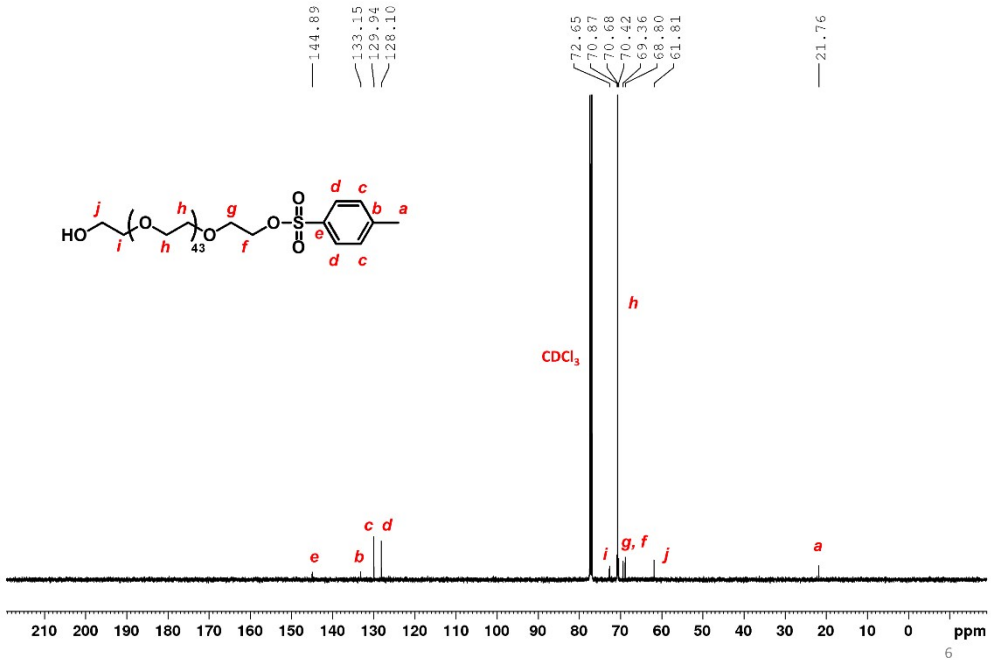

Fig. S2 ^{13}C NMR spectrum of P1.

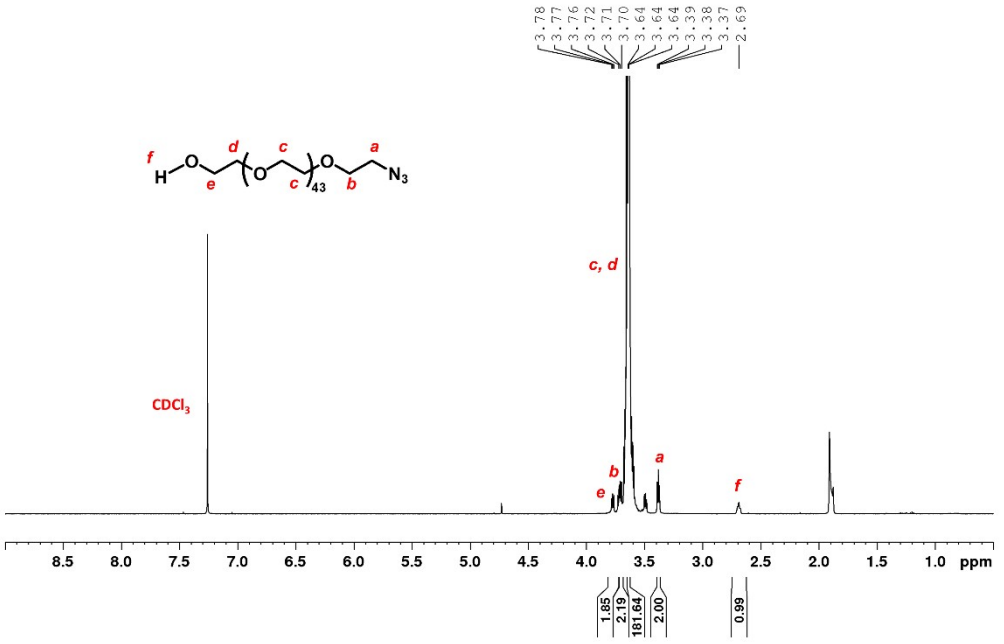

Fig. S3 ^{1}H NMR spectrum of P2.

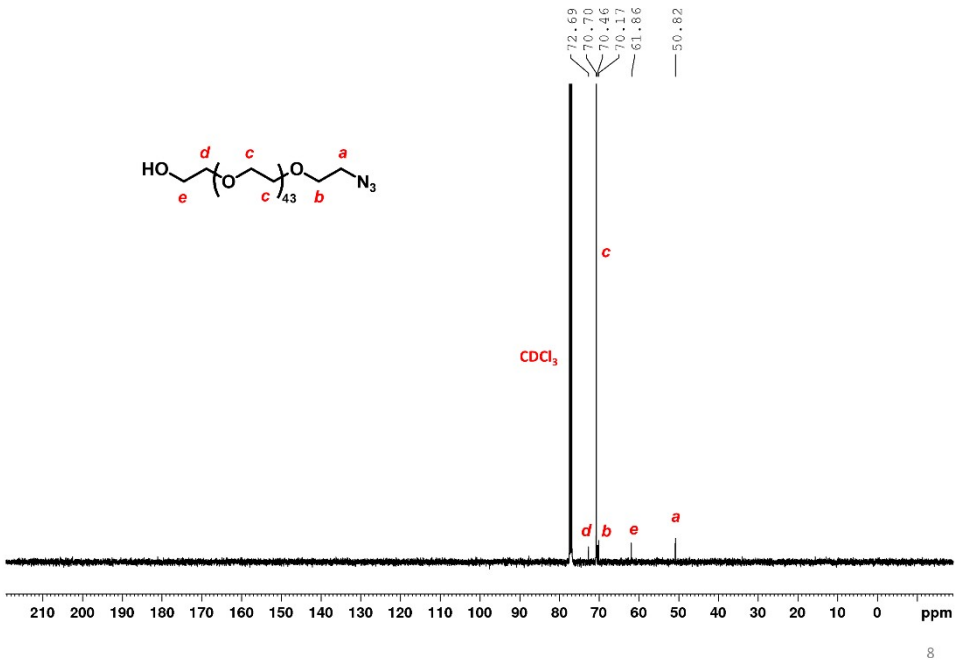

Fig. S4 ^{13}C NMR spectrum of P2.

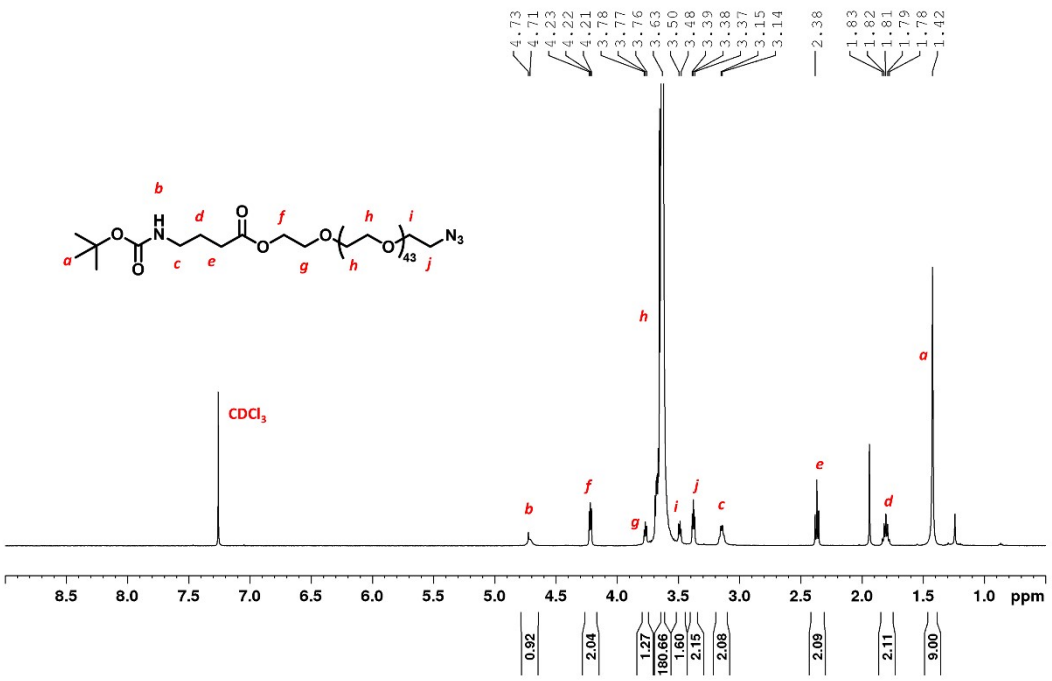

Fig. S5 ^{1}H NMR spectrum of P3.

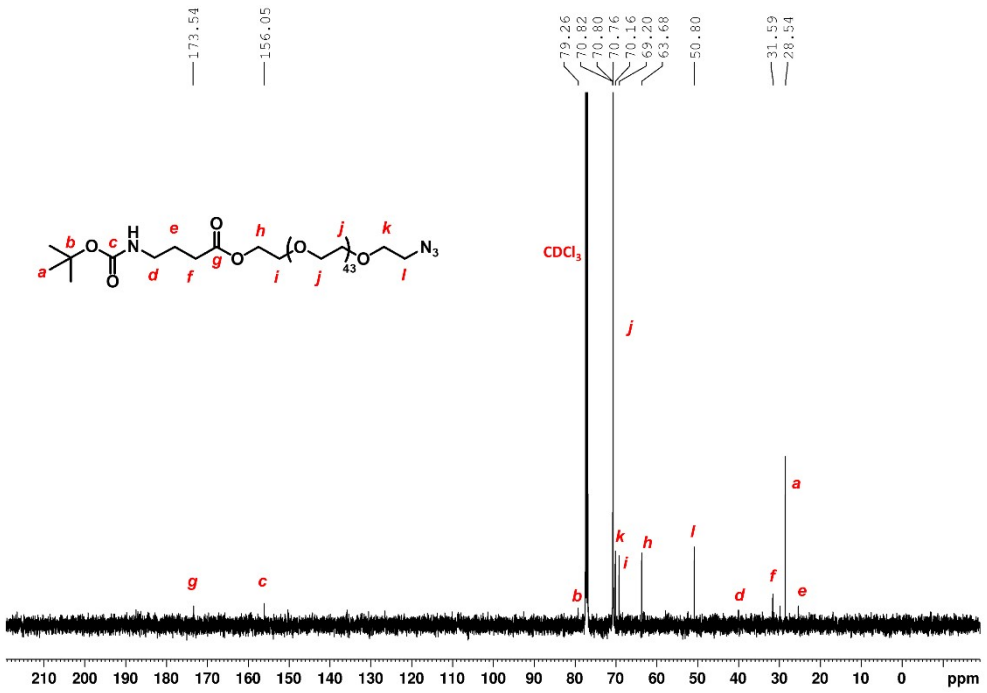

Fig. S6 ^{13}C NMR spectrum of P3.

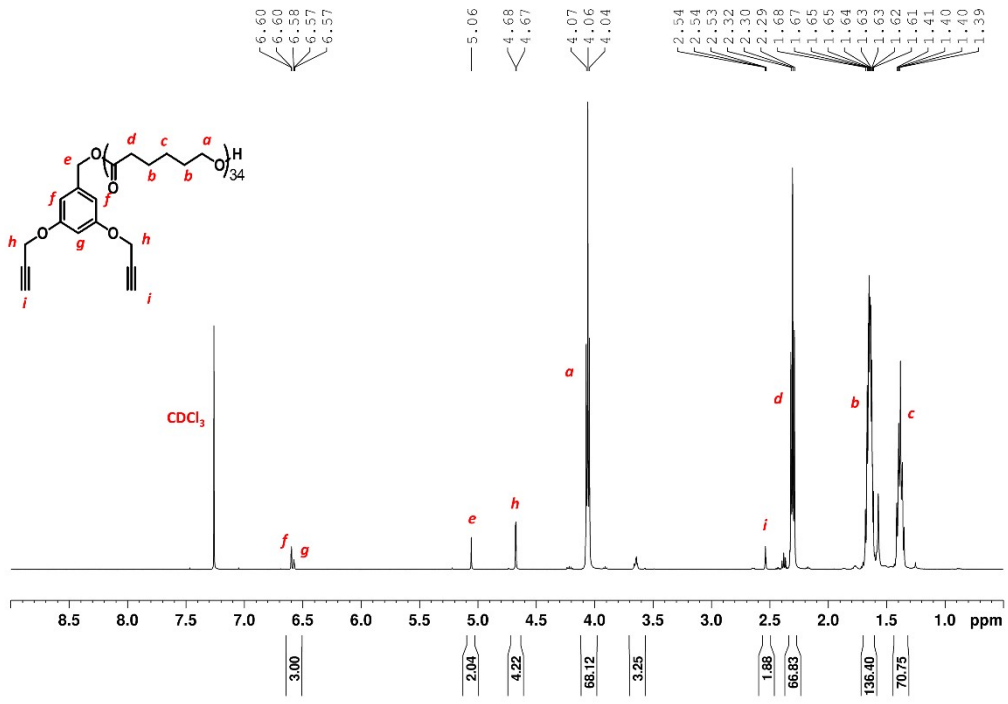

Fig. S7 ^{1}H NMR spectrum of P5.

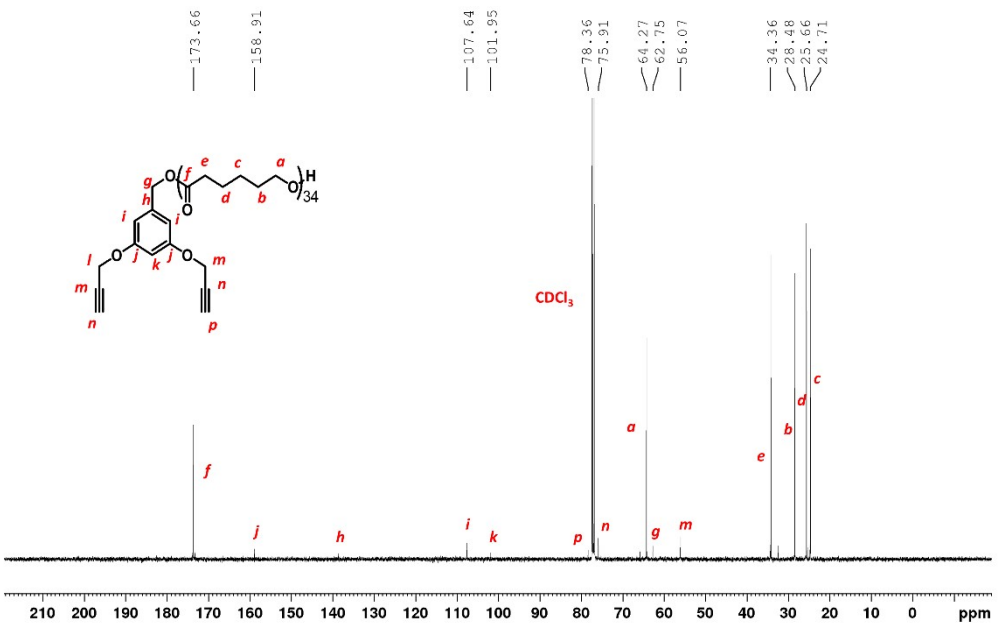

Fig. S8 ^{13}C NMR spectrum of P5.

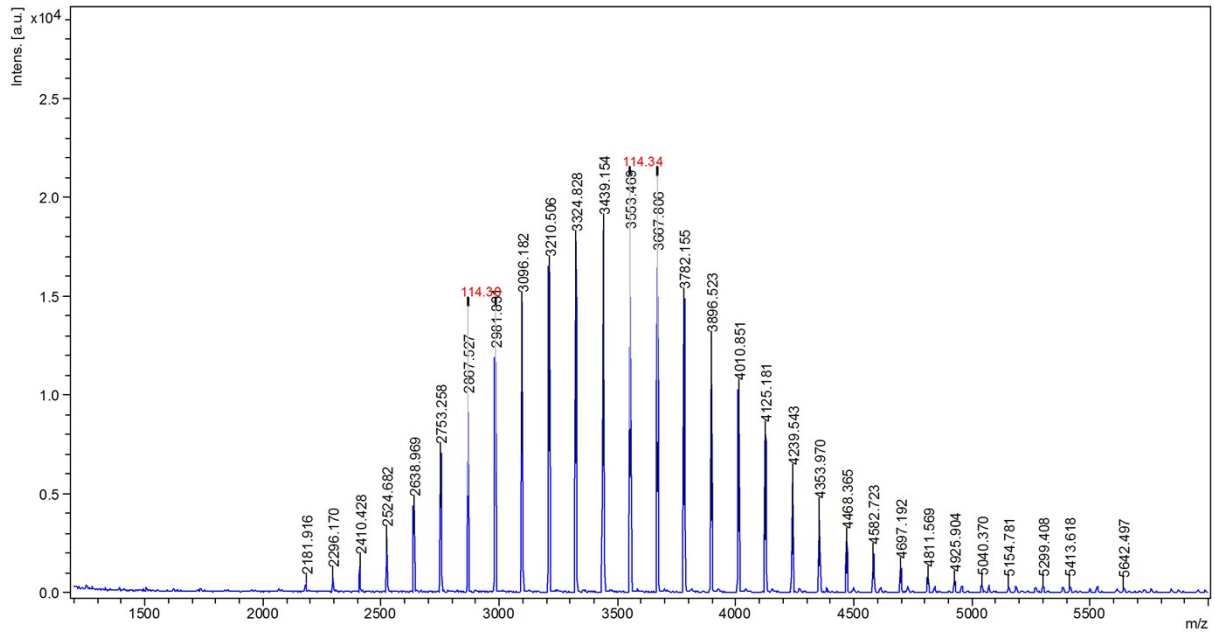

Fig. S9 MALDI-Tof spectrum of P5.

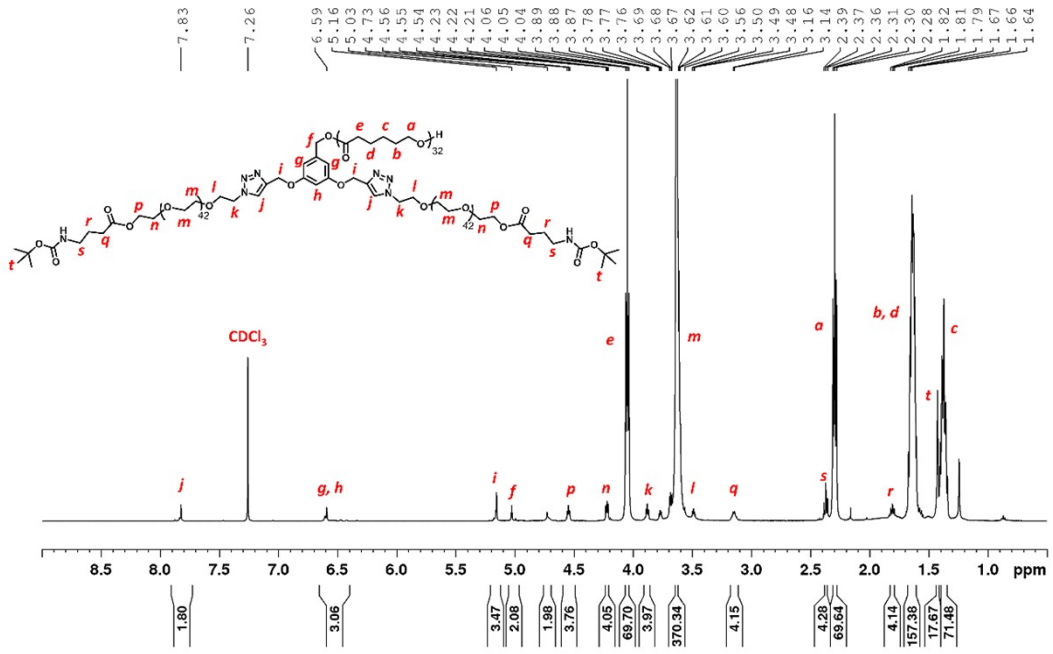

Fig. S10 ^{1}H NMR spectrum of P6.

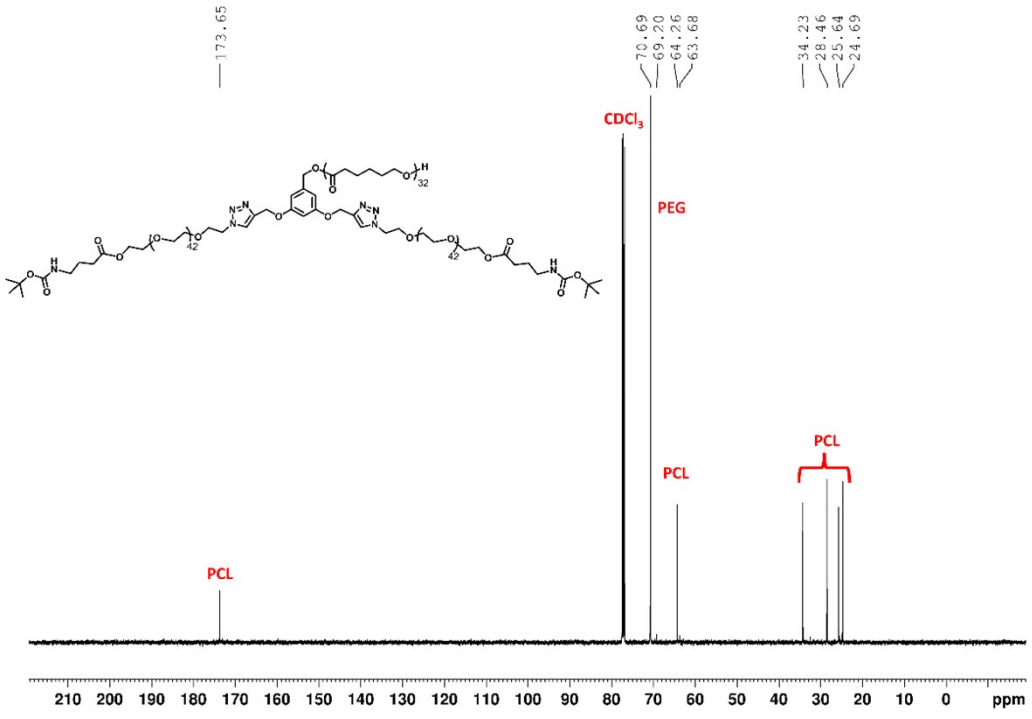

Fig. S11 ^{13}C NMR spectrum of P6.

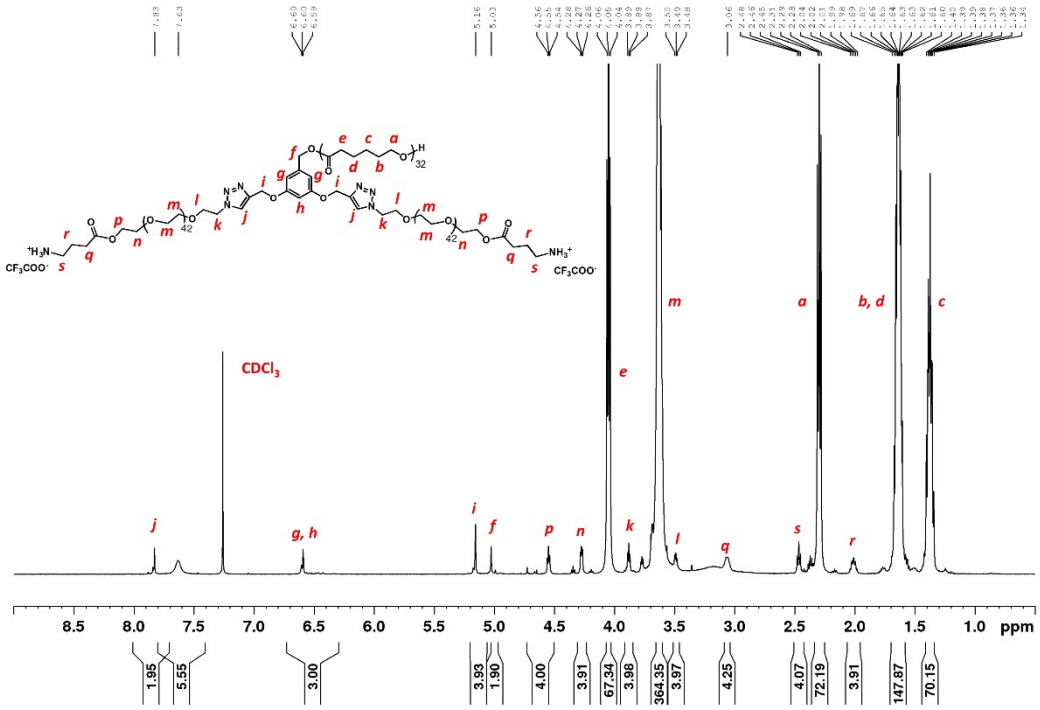

Fig. S12 ^{1}H NMR of P7.

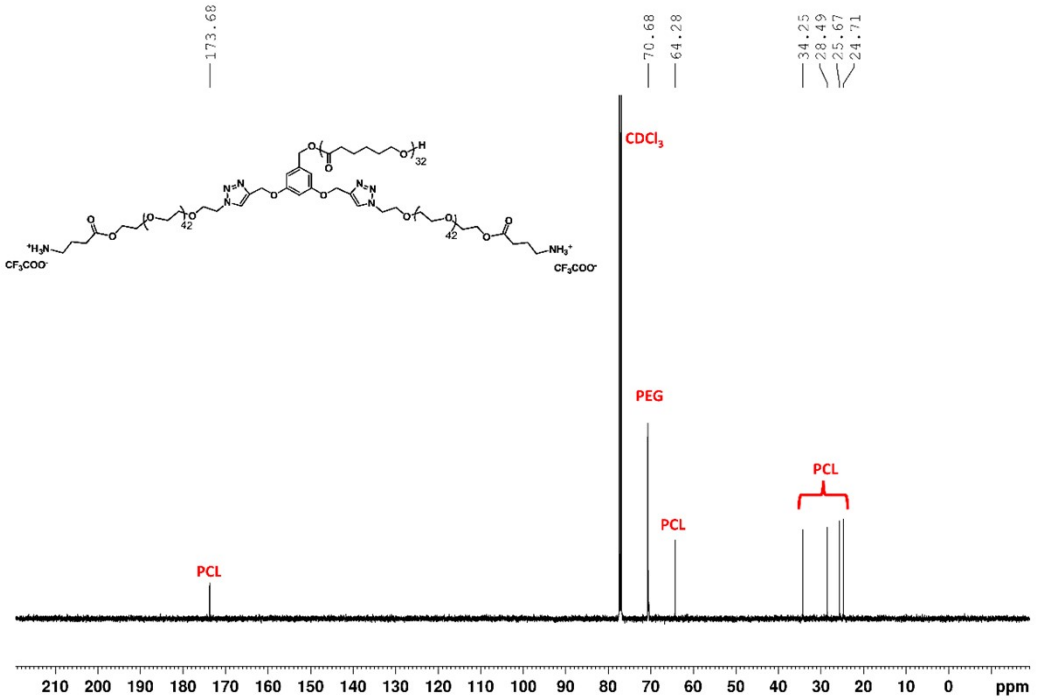

Fig. S13 ^{13}C NMR of P7.

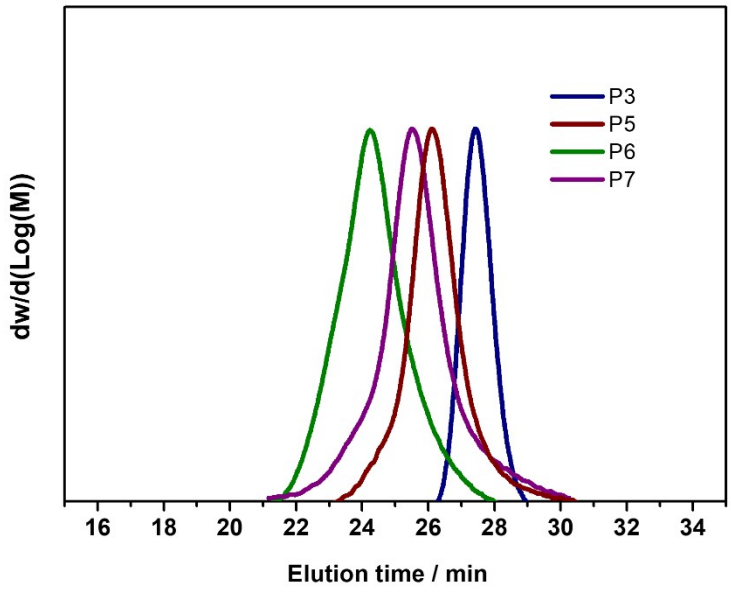

Fig. S14 GPC traces of P3 (blue *Đ*=1.11), P5 (brown, *Đ*=1.26), P6 (green, *Đ*=1.38), and P7 (purple, *Đ*=1.54).

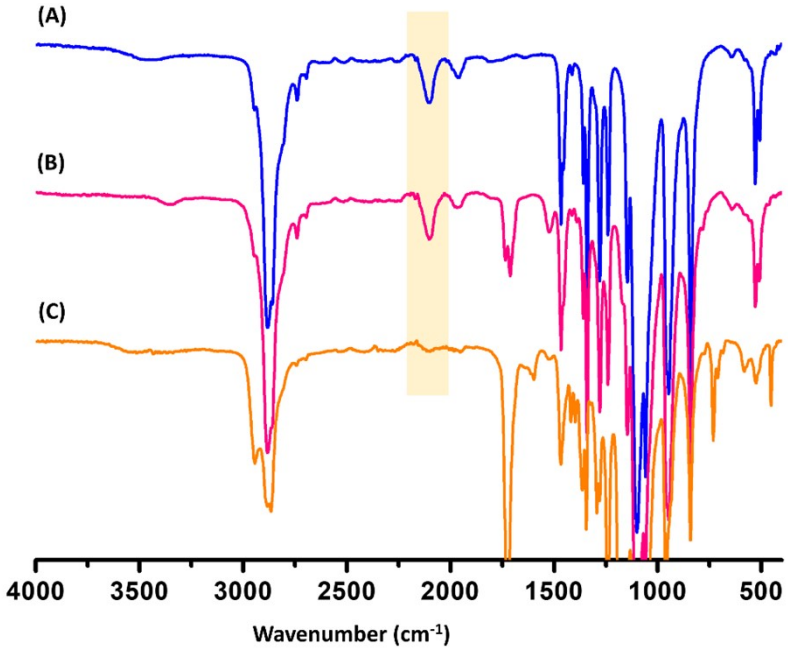

Fig. S15 FTIR spectrum of (A) P2, (B) P3 and (C) P6. The presence of the azide in P2 and P3 was confirmed by the appearance of a peak at 2120 cm^{-1}.

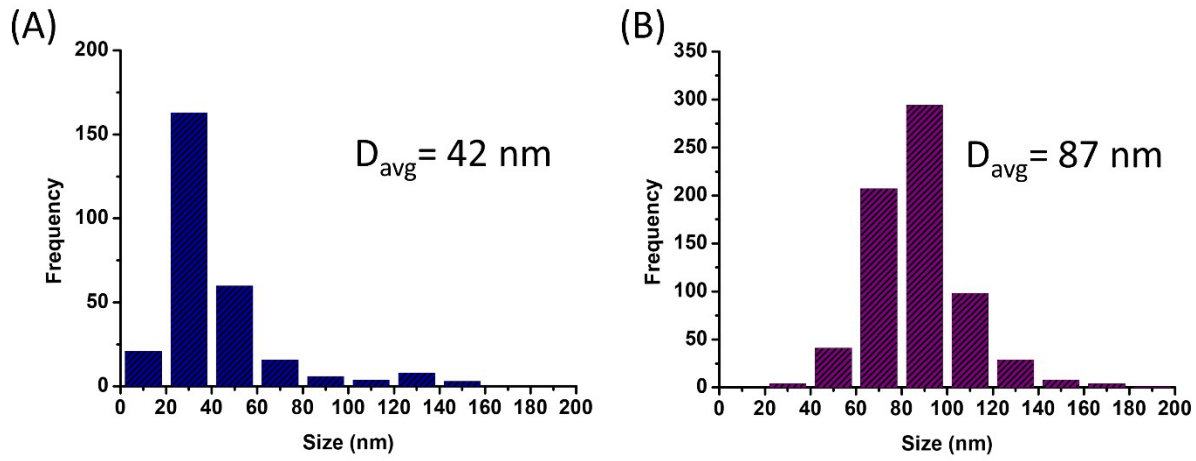

Fig. S16 TEM analyses of (A) P6-micelles and (B) P7-micelles.

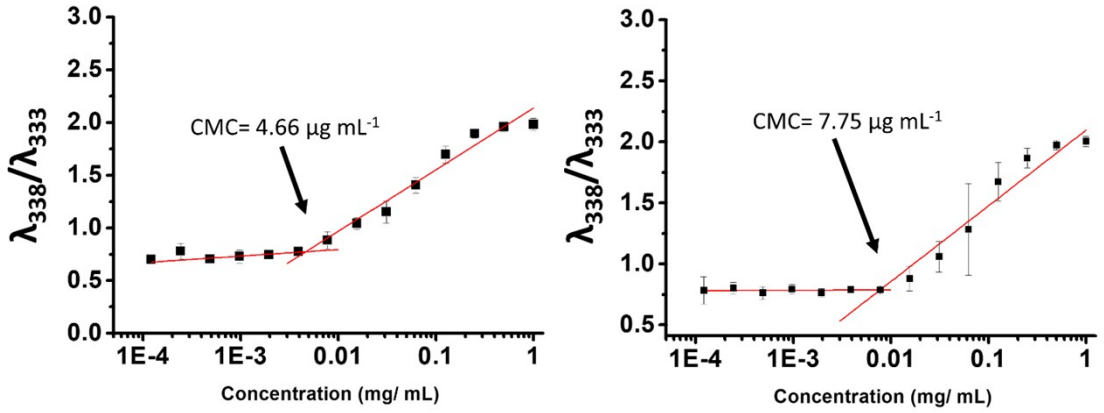

Fig. S17 The CMC of (A) P6-micelles and (B) P7-micelles derived from the plot of fluorescence intensity of pyrene at 338 nm and 333 nm against polymer concentration.

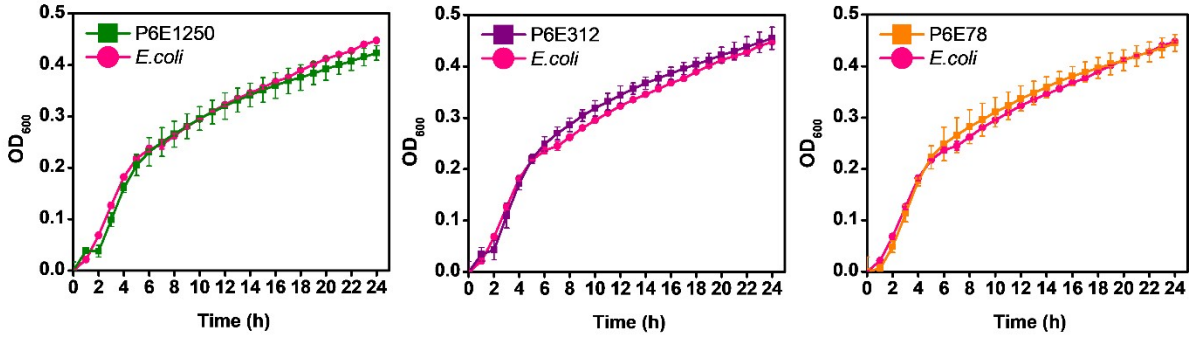

Fig. S18 Growth curve analyses of *E. coli* in the presence of P6-micelles. Graph legends: P6 represents P6-micelles. Letter E following sample represents *E. coli*, while the numbers that follow suit represent concentration of micellar solutions (e.g., P6E1250 contains 1250 μg mL^{-1} of P6-micelle added to *E. coli*).

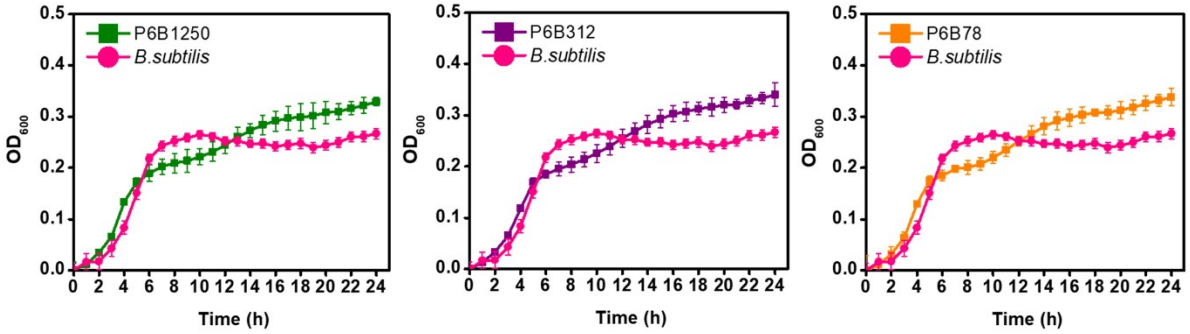

Fig. S19 Growth curve analyses of *B. subtilis* in the presence of P6-micelles. Graph legends: P6 represents P6-micelles. Letter B following sample represents *B. subtilis*, while the numbers that follow suit represent concentration of micellar solutions (e.g., P6B1250 contains 1250 μg mL^{-1} of P6-micelle added to *B. subtilis*).

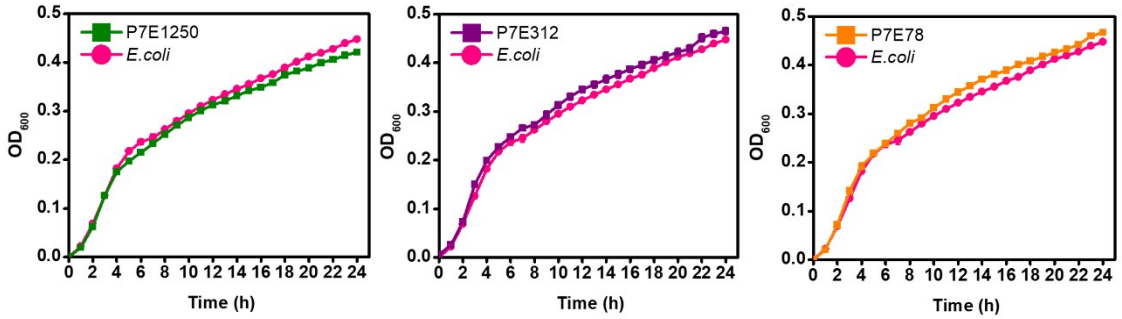

Fig. S20 Growth curve analyses of *E. coli* in the presence of P7-micelles. Graph legends: P6 represents P7-micelles. Letter E following sample represents *E. coli*, while the numbers that follow suit represent concentration of micellar solutions (e.g., P7E1250 contains 1250 μg mL^{-1} of P7-micelle added to *E. coli*).

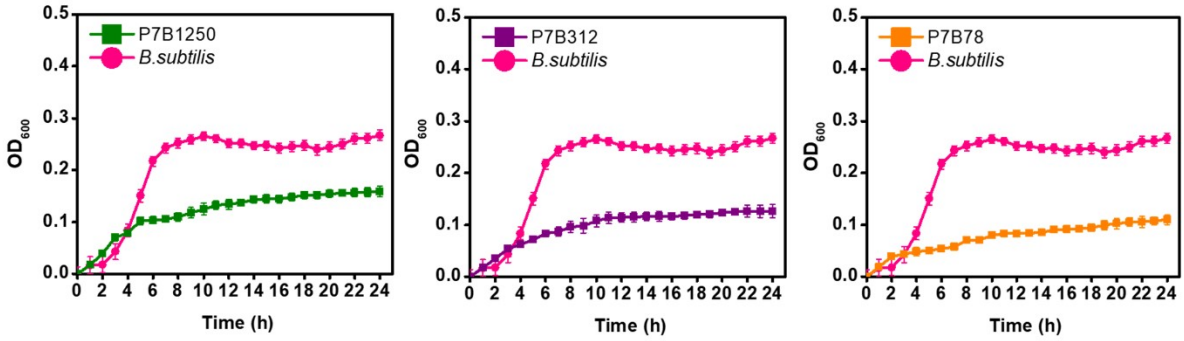

Fig. S21 Growth curve analyses of *B. subtilis* in the presence of P7-micelles. Graph legends: P7 represents P7-micelles. Letter B following sample represents *B. subtilis*, while the numbers that follow suit represent concentration of micellar solutions (e.g., P7B1250 contains 1250 μg mL^{-1} of P7-micelle added to *B. subtilis*).

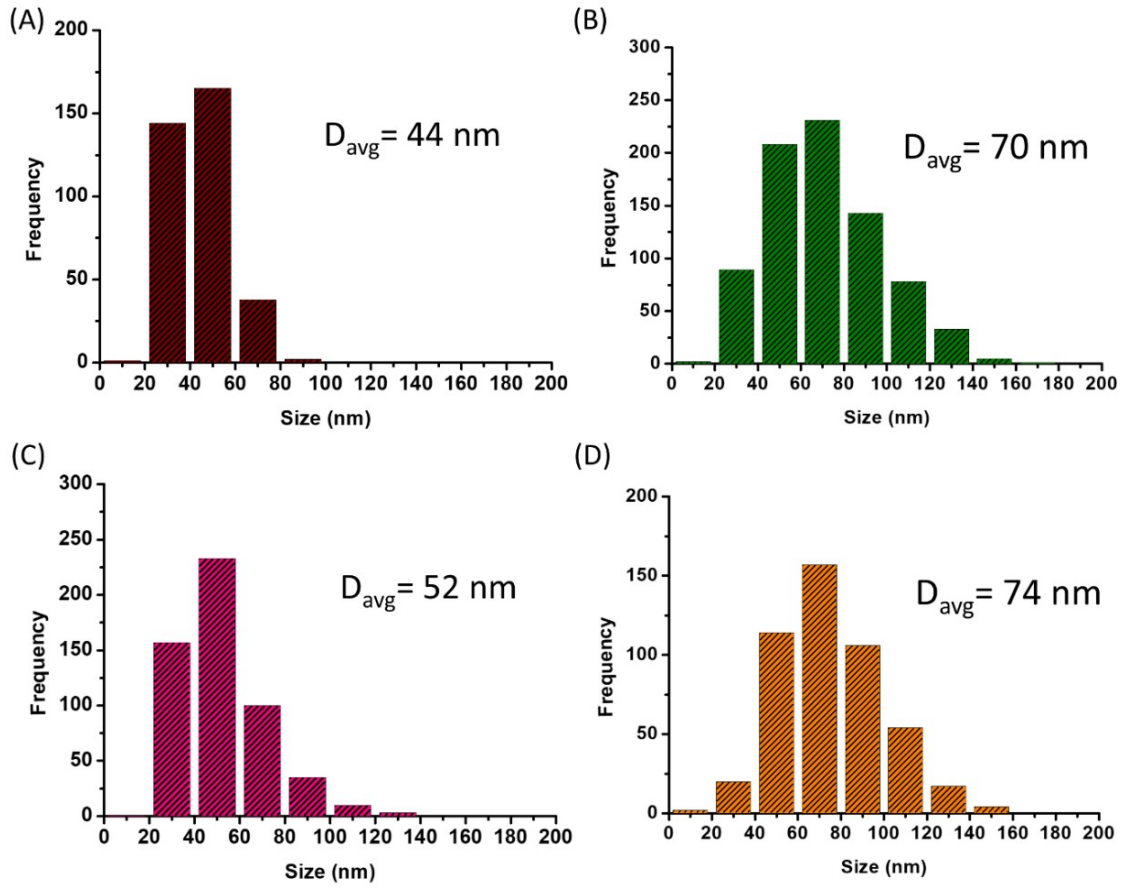

Fig. S22 TEM analyses of (A) P6-CUR, (B) P6-TBF, (C) P7-CUR, and (D) P7-TBF.

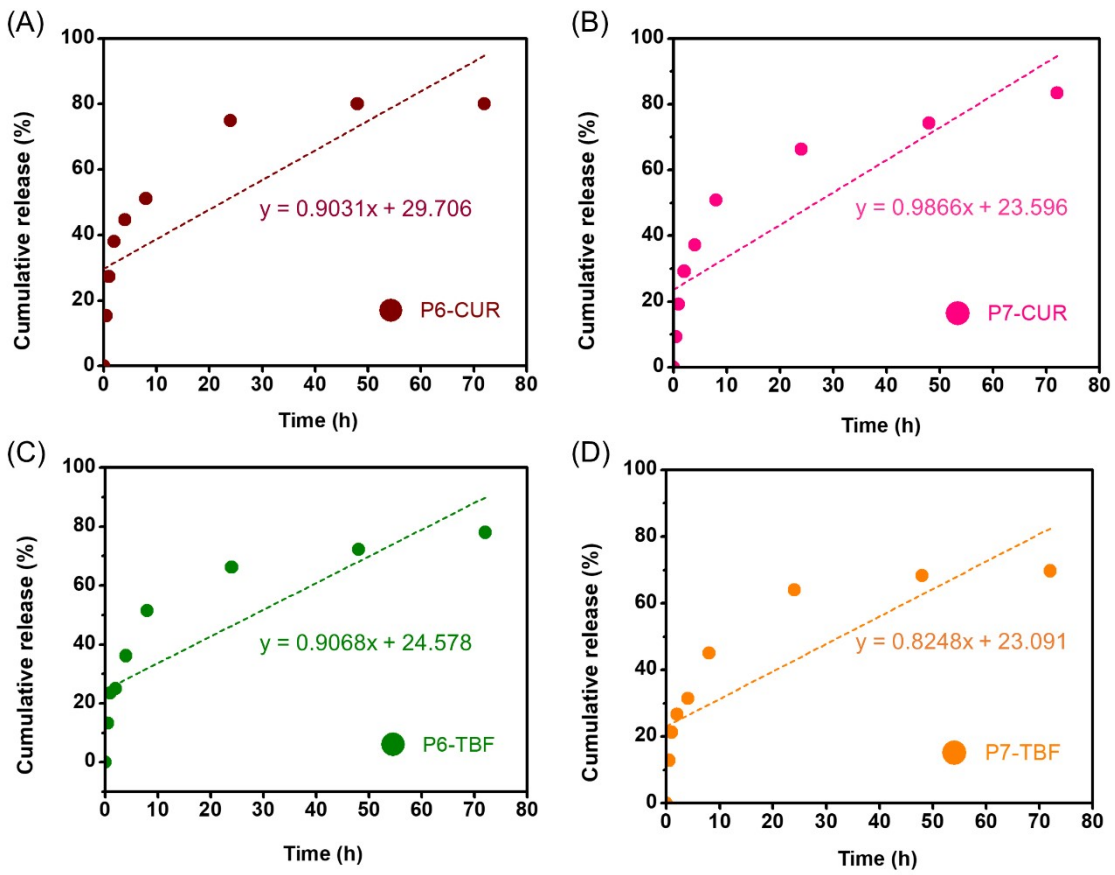

Fig. S23 Drug release data fitted to zero-order model: (A) P6-CUR, (B) P7-CUR, (C) P6-TBF and (D) P7-CUR.

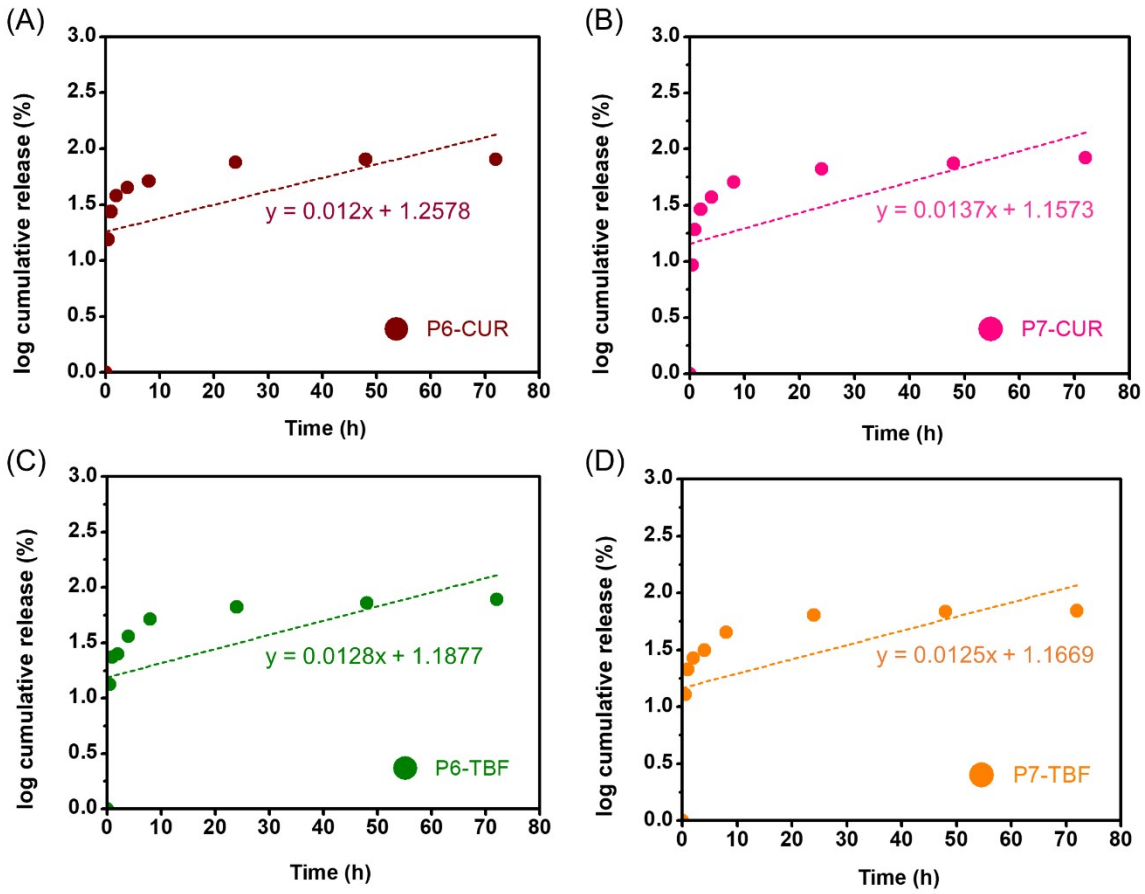

Fig. S24 Drug release data fitted to first-order model: (A) P6-CUR, (B) P7-CUR, (C) P6-TBF and (D) P7-CUR.

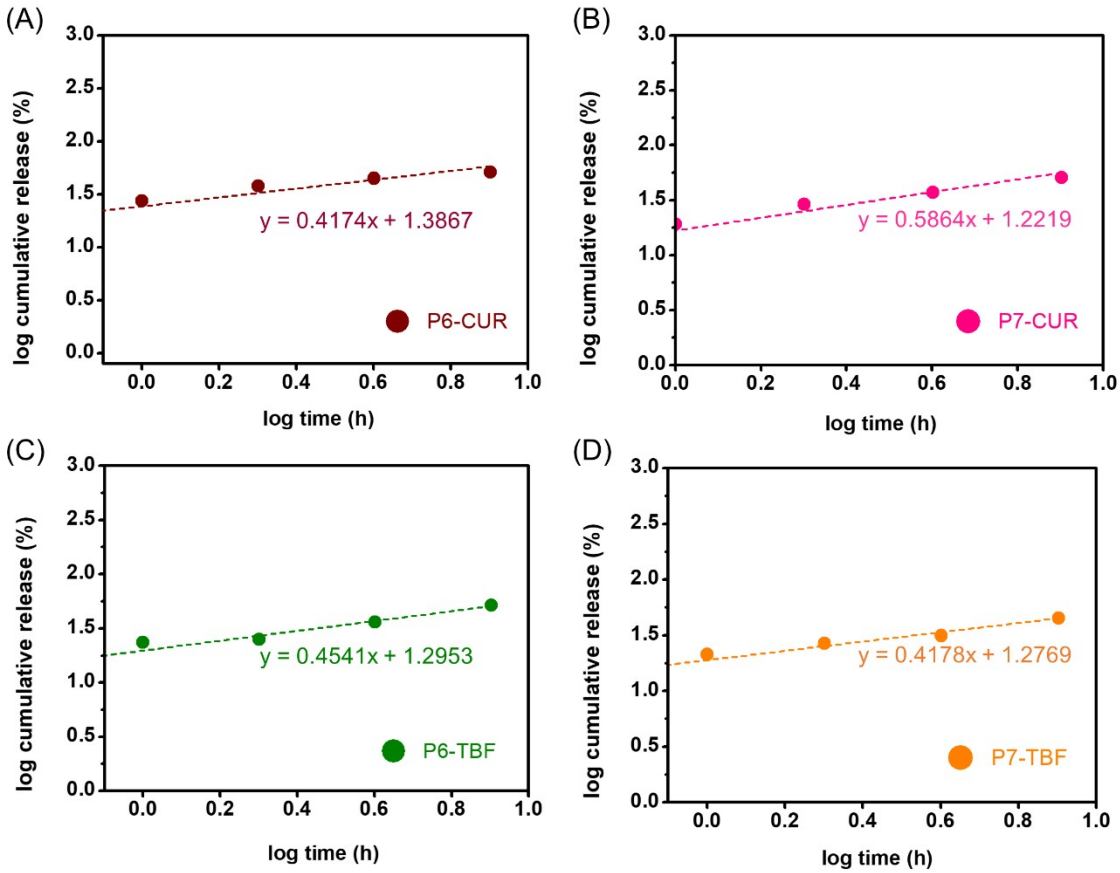

Fig. S25 Drug release data fitted to Korsmeyer-Peppas model: (A) P6-CUR, (B) P7-CUR, (C) P6-TBF and (D) P7-CUR.

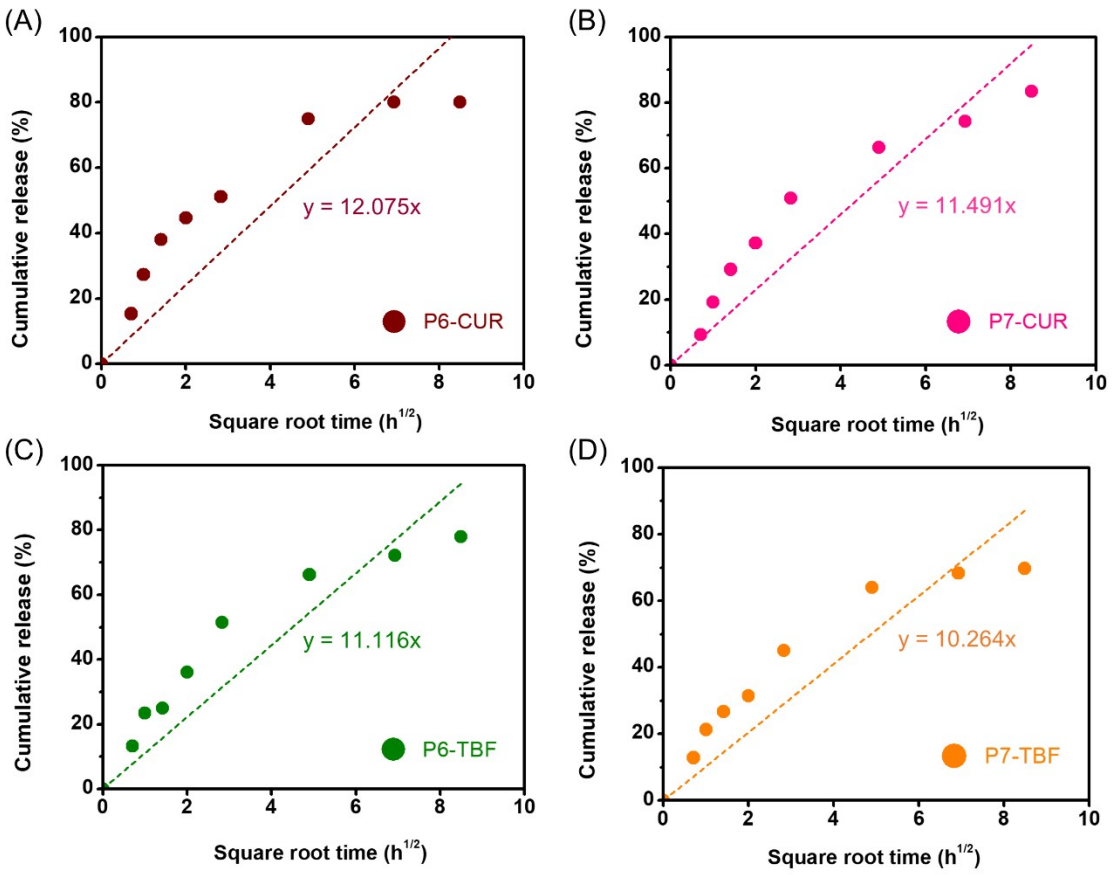

Fig. S26 Drug release data fitted to Higuchi model: (A) P6-CUR, (B) P7-CUR, (C) P6-TBF and (D) P7-CUR.

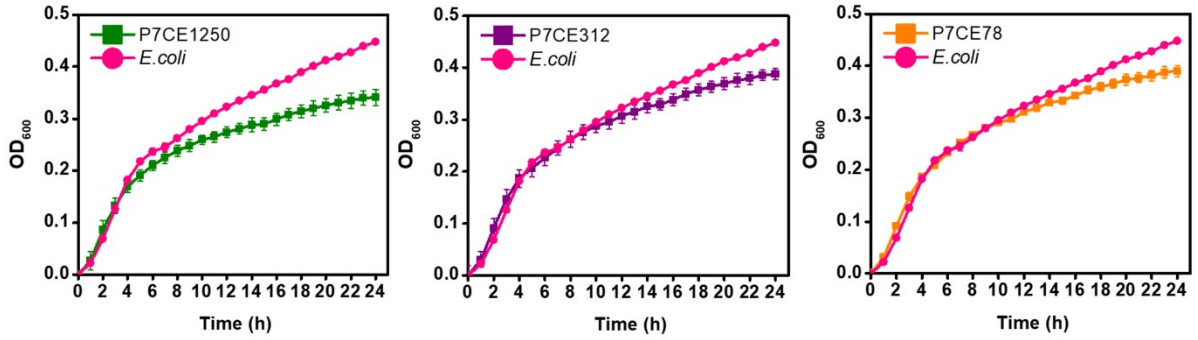

Fig. S27 Growth curve analyses of *E. coli* in the presence of P7-CUR. Graph legends: P7C represents P7-CUR. Letter E following sample represents *E. coli*, while the numbers that follow suit represent concentration of micellar solutions (e.g., P7CE1250 contains 1250 μg mL^{-1} of P7-CUR added to *E. coli*).

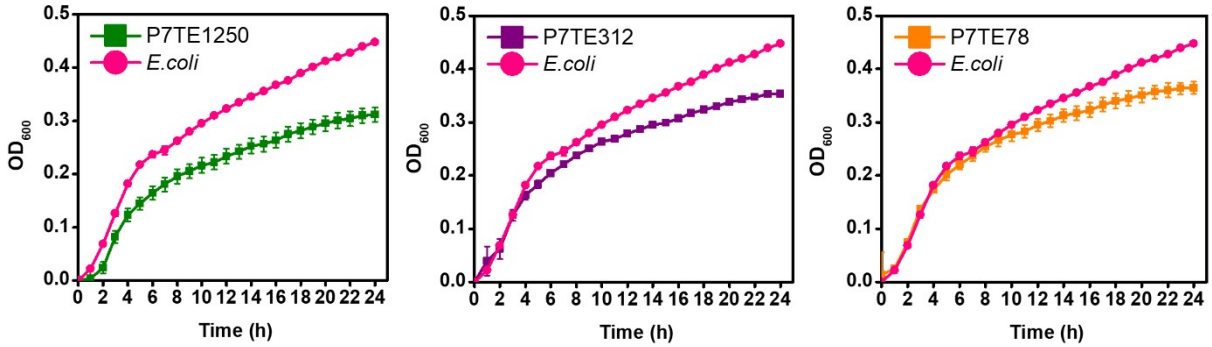

Fig. S28 Growth curve analyses of *E. coli* in the presence of P7-TBF. Graph legends: P7T represents P7-TBF. Letter E following sample represents *E. coli*, while the numbers that follow suit represent concentration of micellar solutions (e.g., P7TE1250 contains 1250 μg mL^{-1} of P7-TBF added to *E. coli*).

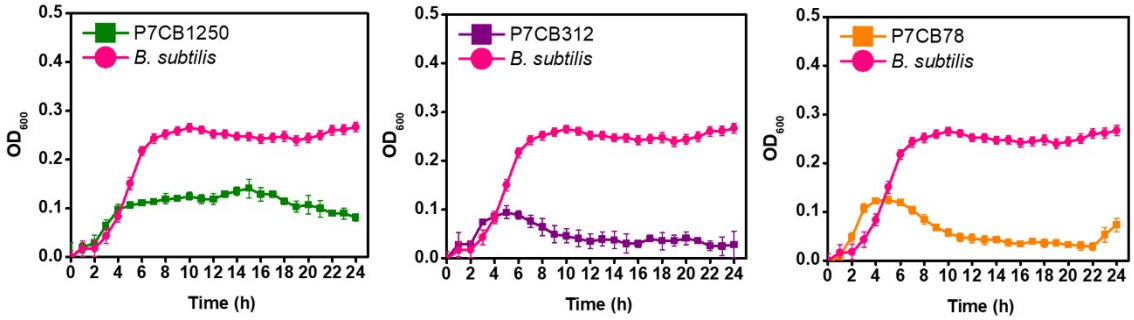

Fig. S29 Growth curve analyses of *B. subtilis* in the presence of P7-CUR. Graph legends: P7C represents P7-CUR. Letter B following sample represents *B. subtilis*, while the numbers that follow suit represent concentration of micellar solutions (e.g., P7CB1250 contains 1250 µg mL^{-1} of P7-CUR added to *B. subtilis*).

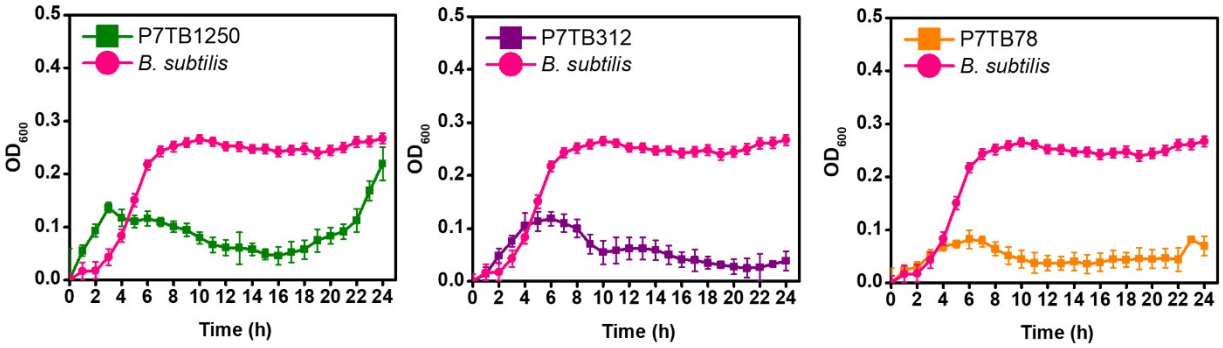

Fig. S30 Growth curve analyses of *B. subtilis* in the presence of P7-TBF. Graph legends: P7T represents P7-TBF. Letter B following sample represents *B. subtilis*, while the numbers that follow suit represent concentration of micellar solutions (e.g., P7TB1250 contains 1250 µg mL^{-1} of P7-TBF added to *B. subtilis*).

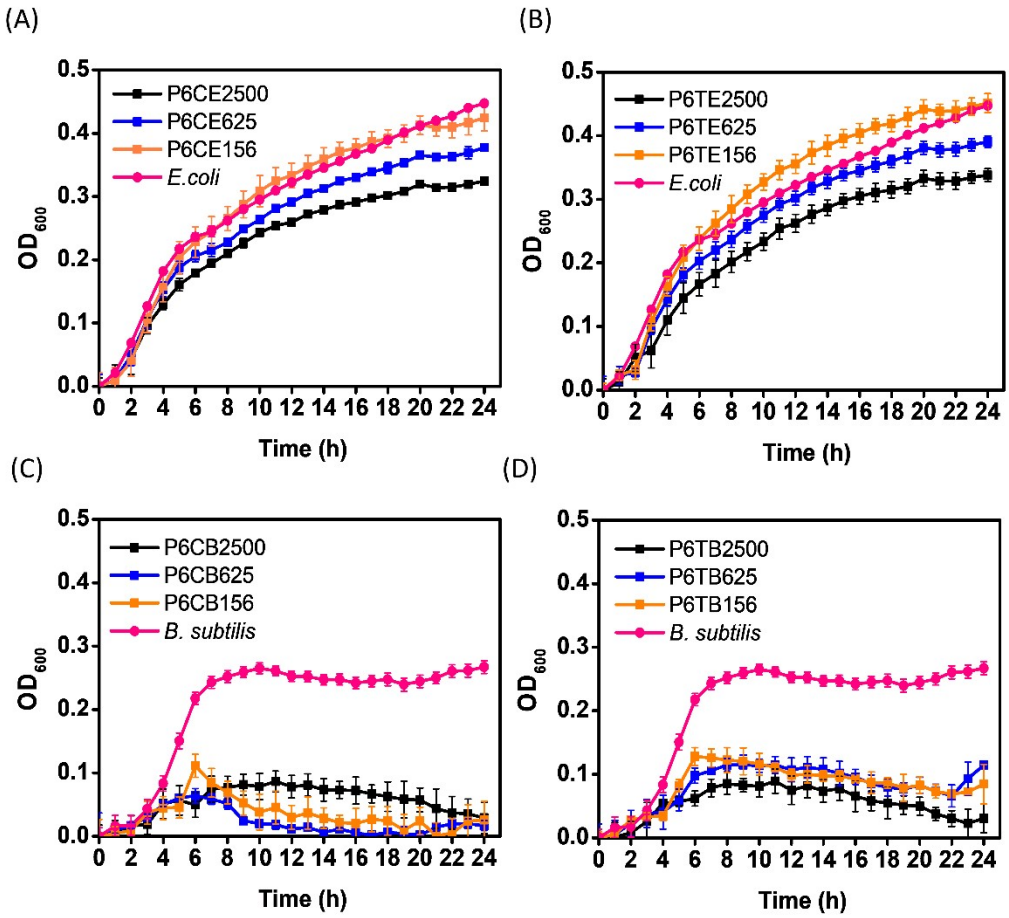

Fig. S31 Growth curves of *E. coli* treated with (A) P6-CUR and (B) P6-TBF, and *B. subtilis* treated with (C) P6-CUR and (H) P6-TBF. Graph legends: P6C represents P6-CUR whereas P6T represents P6-TBF. Letter following sample represents bacterial strains, while the numbers that follow suit represent concentration of micellar solutions (e.g., P6CE2500 contains 2500 μg mL^{-1} of P6-CUR added to *E. coli*, P6TB2500 contains 2500 μg mL^{-1} of P6-TBF added to *B. subtilis*). For additional concentrations tested, see Figure S32-35.

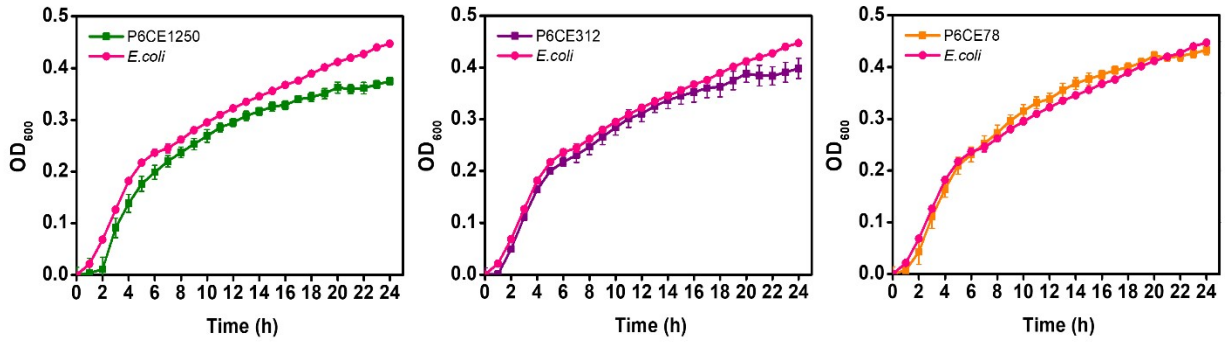

Fig. S32 Growth curve analyses of *E. coli* in the presence of P6-CUR Graph legends: P6C represents P6-CUR. Letter E following sample represents *E. coli*, while the numbers that follow suit represent concentration of micellar solutions (e.g., P6CE 1250 contains 1250 µg mL^{-1} of P6-CUR added to *E. coli*).

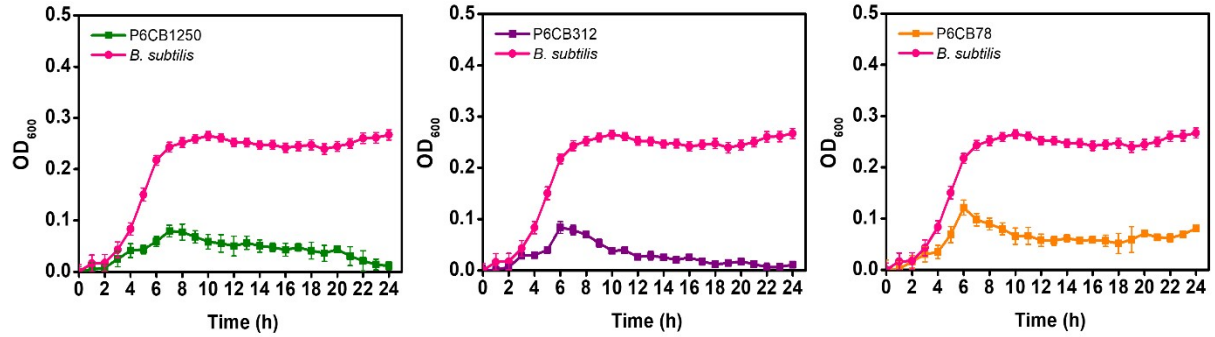

Fig. S33 Growth curve analyses of *B. subtilis* in the presence of P6-CUR. Graph legends: P6C represents P6-CUR. Letter B following sample represents *B. subtilis*, while the numbers that follow suit represent concentration of micellar solutions (e.g., P6CB1250 contains 1250 µg mL^{-1} of P6- CUR added to *B. subtilis*).

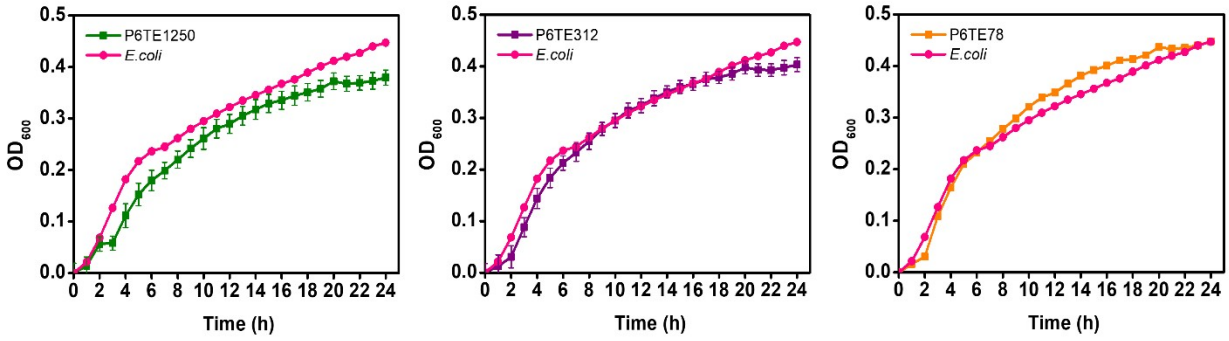

Fig. S34 Growth curve analyses of *E. coli* in the presence of P6-TBF. Graph legends: P6T represents P6-TBF. Letter E following sample represents *E. coli*, while the numbers that follow suit represent concentration of micellar solutions (e.g., P6TE1250 contains 1250 μg mL^{-1} of P6-TBF added to *E. coli*).

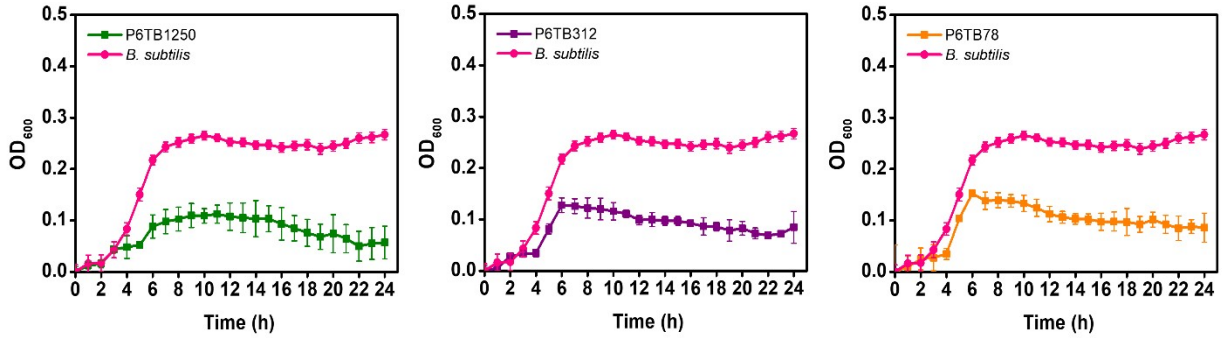

Fig. S35 Growth curve analyses of *B. subtilis* in the presence of P6-TBF. Graph legends: P6T represents P6-TBF. Letter B following sample represents *B. subtilis*, while the numbers that follow suit represent concentration of micellar solutions (e.g., P6TB1250 contains 1250 μg mL^{-1} of P6-TBF added to *B. subtilis*).

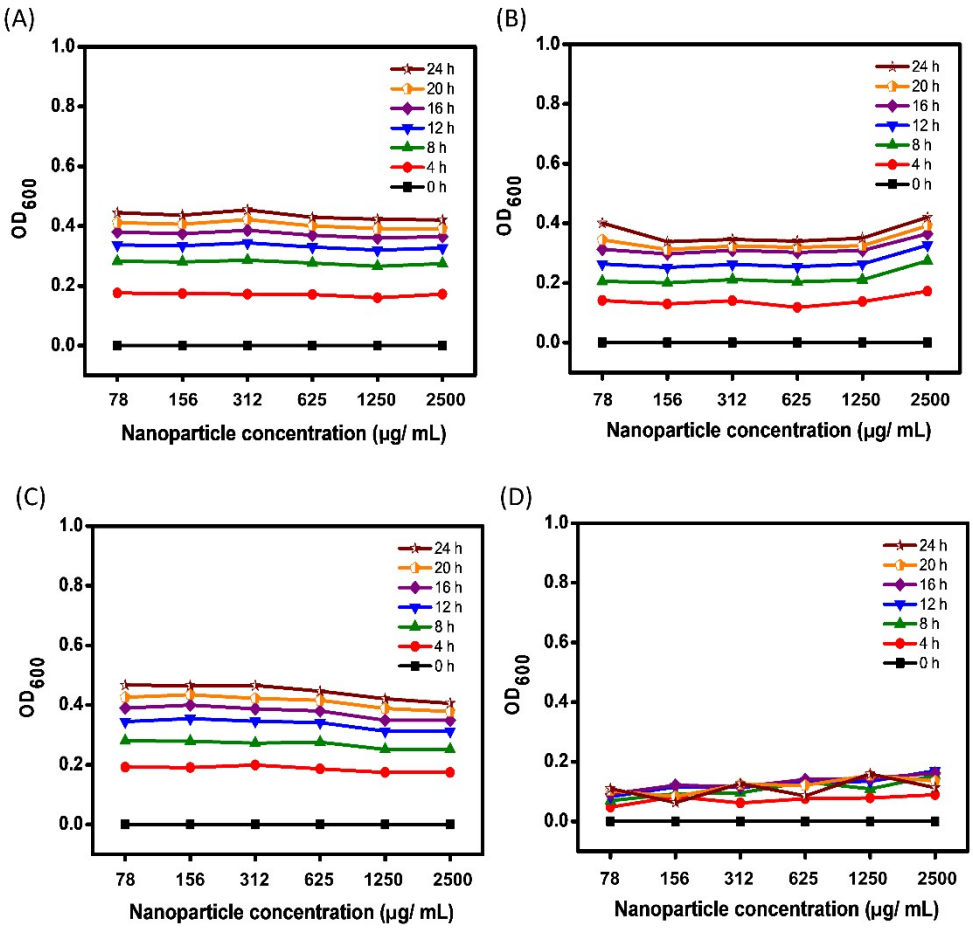

Fig. S36 Optical density (at 600 nm) analyses of samples at various time intervals with respect to nanoparticle concentrations: (A) P6-micelles against *E. coli*, (B) P6-micelles against *B. subtilis*, (C) P7-micelles against *E. coli*, (D) P7-micelles against *B. subtilis*.

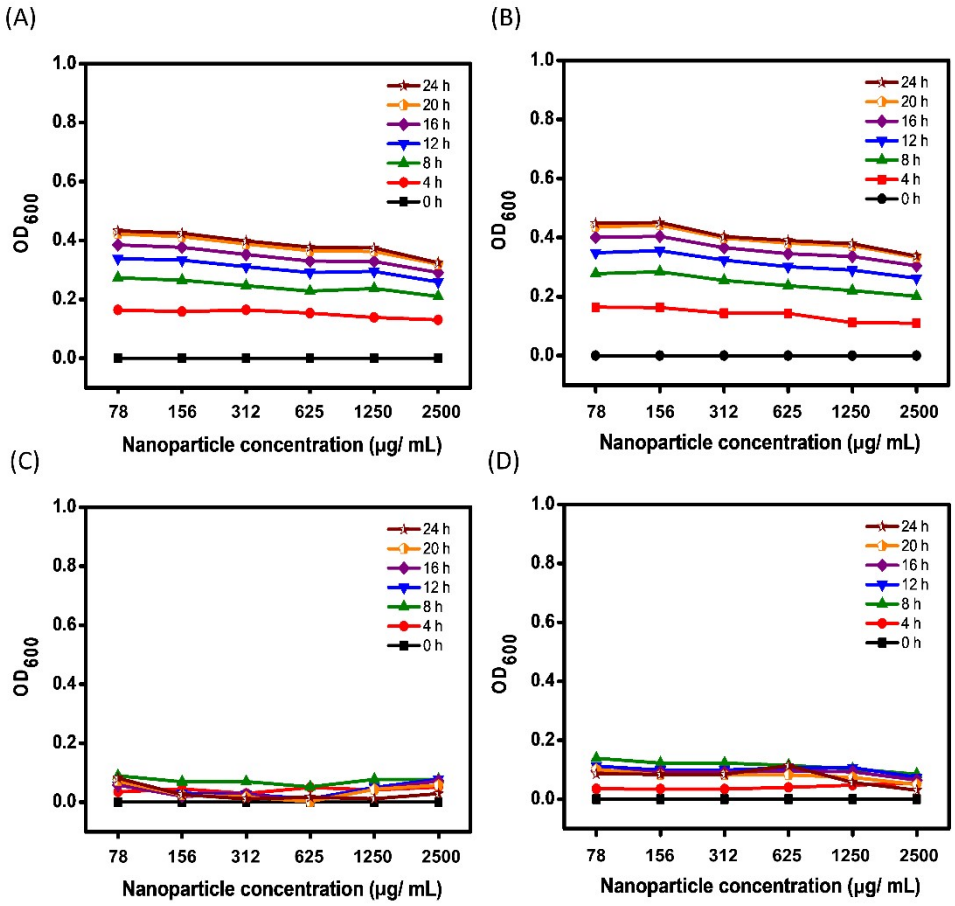

Fig. S37 Optical density (at 600 nm) analyses of samples at various time intervals with respect to nanoparticle concentrations: (A) P6-CUR against *E. coli*, (B) P6-TBF against *E. coli*, (C) P6-CUR-micelles against *B. subtilis*, (D) P6-TBF against *B. subtilis*.

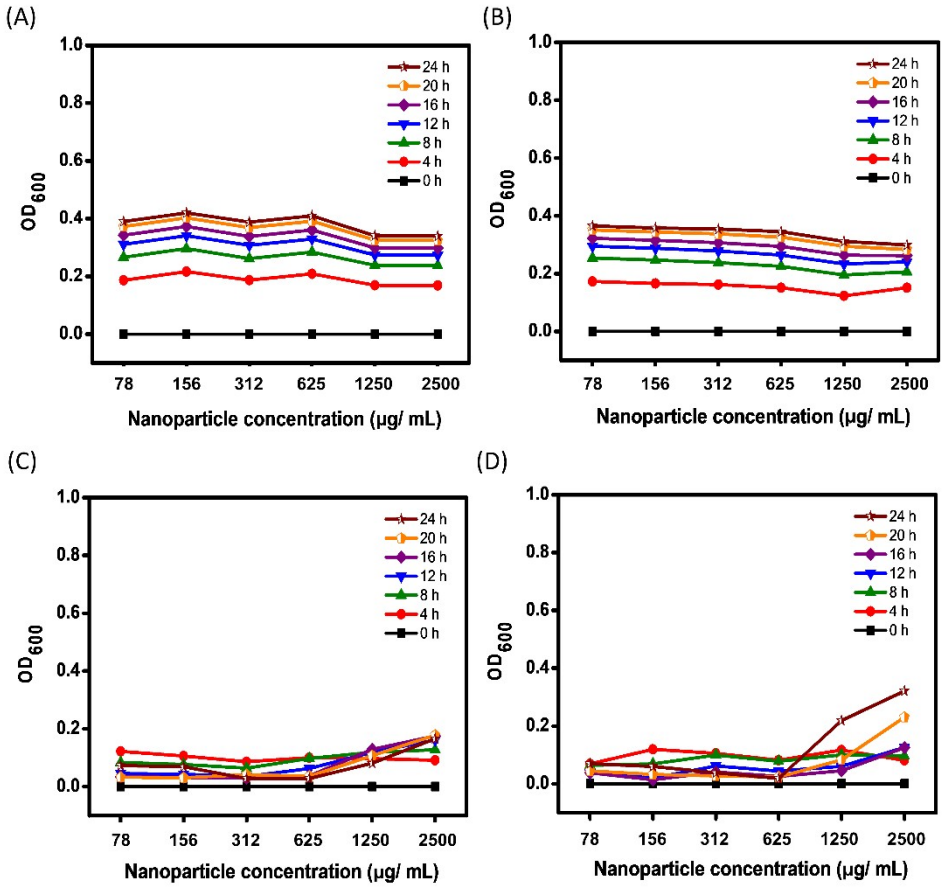

Fig. S38 Optical density (at 600 nm) analyses of samples at various time intervals with respect to nanoparticle concentrations: (A) P7-CUR against *E. coli*, (B) P7-TBF against *E. coli*, (C) P7-CUR-micelles against *B. subtilis*, (D) P7-TBF against *B. subtilis*.